The Utilization of *Gracilaria* sp. as Raw Material for Cellulose in Cellulose Acetate-Nickel Oxide (CA-NiO) as Electrode for Energy Storage Technology

Abdul Karim[1], Ahyar Ahmad[1,2,3*], Rugaiyah Andi Arfah[1], Riksfardini Annisa Ermawar[4], Harningsih Karim[5], Andi Erwin Eka Putra[6], Suriati Eka Putri[7], Satria Putra Jaya Negara[7], and Siti Halimah Larekeng[3,8,9]

[1]*Department of Chemistry, Faculty of Mathematics and Natural Sciences, Hasanuddin University, Jl. Perintis Kemerdekaan Km. 10, Makassar 90245, Indonesia*

[2]*Research and Development Center for Biopolymers and Bioproducts, LPPM, Hasanuddin University, Jl. Perintis Kemerdekaan Km. 10, Makassar 90245, Indonesia*

[3]*Research Collaboration Center for KARST Microbes BRIN-LPPM, Hasanuddin University, Jl. Perintis Kemerdekaan Km. 10, Makassar 90245, Indonesia*

[4]*Research Center for Biomass and Bioproducts, National Research and Innovation Agency (BRIN), Jl. Raya Jakarta Bogor Km. 46, Cibinong 16911, Indonesia*

[5]*Department of Pharmacy, School of Pharmacy YAMASI, Jl. Mapala 2 Blok D5 No. 10, Makassar 90222, Indonesia*

[6]*Department Mechanical Engineering, Faculty of Engineering, Hasanuddin University, Jl. Poros Malino Km. 5, Gowa 92171, Indonesia*

[7]*Department of Chemistry, Faculty of Mathematics and Natural Sciences, Universitas Negeri Makassar, Jl. Daeng Tata, Makassar 90244, Indonesia*

[8]*KARST Bioprospecting and Society Research Group, Hasanuddin University, Jl. Perintis Kemerdekaan Km. 10, Makassar 90245, Indonesia*

[9]*Faculty of Forestry, Hasanuddin University, Jl. Perintis Kemerdekaan Km. 10, Makassar 90245, Indonesia*

**** Corresponding author:***

tel: +62-8984917549
email: ahyarahmad@gmail.com

Received: May 28, 2024
Accepted: October 16, 2024

DOI: 10.22146/ijc.96533

Abstract: *In the modern era, electrical energy has become a significant need that drives the large consumption of fossil fuels and their environmental impacts. Supercapacitors can reduce this large consumption of natural polymers such as cellulose acetate (CA), which can be synthesized from* Gracilaria *sp. Composites with CA can be an environmentally friendly alternative electrode with low toxicity. The results show that the cellulose has been successfully synthesized from the algae* Gracilaria *sp., which was proven by FTIR spectra analysis. The results also show that supercapacitor electrodes have been successfully made where the manufactured electrodes form a composite between CA and nickel oxide (NiO), with the highest specific capacitance and specific energy values of* 15.5×10^2 *F/g and* 13.3×10^2 *Wh/kg, respectively, on the CA-*NiO_2 *electrode, but when the NiO concentration is higher than the CA concentration the specific capacitance and specific energy decrease as shown on the CA-NiO electrode with NiO mass of 0.6 g. Thus, the materials results of this study can be applied to electric vehicles and technology that requires electricity storage in the future.*

Keywords: *cellulose acetate; energy storage;* Gracilaria *sp.; nickel oxide*

■ INTRODUCTION

The requirement for electrical energy in modern life has grown significantly [1], which has led to high use of fossil fuels and an increase in environmental degradation [2-3]. As an energy storage technology, batteries can reduce fossil fuel use. However, batteries have a reasonably small power density, are heavy, heat quickly, are toxic, and require quite a long time to charge [4]. Supercapacitors, as an energy storage technology, present a viable solution due to their distinct advantages over batteries, including resistance to high temperatures, high energy density, rapid charging capabilities, and environmental friendliness [5-6].

Since natural polymers have special qualities in terms of power and service life that can last a long time and are environmentally friendly, they can be a promising substitute for creating supercapacitors as efficient energy storage devices [7]. It has attracted the attention of the government and academic researchers to create energy storage devices with high capacity, especially from natural-based biomaterial sources [8]. Due to the presence of polar groups with unpaired electrons in their ionic conductivity, research on supercapacitors utilizing natural polymers like cellulose acetate (CA) has shown promise as an energy storage material while also maintaining a low specific capacitance as an electrode material [9].

CA can be synthesized from cellulose. CA may be effectively processed into membranes, films, and fibers and is inexpensive to produce. It also has strong mechanical stability and is non-toxic [10]. Many plants have the potential to produce cellulose, such as water hyacinth [11], empty fruit bunches of oil palm [12], banana tree fronds [13], seaweed *Eucheuma spinosum*, and seaweed *Gracilaria* sp. [14], seaweed has 9–34% dry weight of extractable cellulose [15]. Sinjai Regency, South Sulawesi, is one province in Indonesia that has a large production of seaweed, especially the *Gracilaria* sp.

Adding metal oxides to CA composite electrode films shows altered structure and morphology. Adding metal oxide to the electrode film may increase the surface area and electron mobility, allowing it to store large amounts of energy [16-17]. The investigation using nickel oxide (NiO) as an additional material for supercapacitor electrodes has also been studied, and it shows a high specific capacity. Al Kiey and Hasanin [18], adding NiO to porous carbon fiber as a supercapacitor electrode increased the particular capacitance by 811 F/g at a current density of 1 A/g after 1000 cycles. Navale et al. [19], adding NiO to polyaniline (Pani) as a hybrid electrode, showed a specific capacity of 936 F/g at a current density of 1 A/g after 2000 cycles. Nunes et al. [20] added NiO to carbon nanotubes as a hybrid electrode, showing a specific capacity of 1200 F/g at a current density of 5 A/g. In this study, we use *Gracilaria* sp. as raw material for CA synthesis, which will be composited with NiO. Its application for electrodes showed a high specific capacity of 15.5×10^2 F/g on maximum conditions. To the best of the authors' knowledge, no previous research has examined the employed cellulose seaweed as an electrode material for future energy storage applications.

■ EXPERIMENTAL SECTION

Materials

The material used in this study was *Gracilaria* sp., which was obtained from Sinjai Regency, South Sulawesi. The materials such as NaOH (Merck), H_2O_2 (Merck), CH_3COOH (Merck), Na_2SO_4 (Merck), NiO nanoparticle (Sigma-Aldrich), and dibutyl phthalate (DBP, Merck) were also used in this study.

Instrumentation

The instruments used in this study are an FTIR spectrophotometer (Prestige-21, Shimadzu), Scanning Electron Microscope (SEM, JEOL-6000PL), and X-ray diffraction (XRD, Shimadzu 7000), and Cyclic Voltammetry (CV, CS350M EIS Potentiostat, Wuhan, Cina).

Procedure

Sample preparation

The first step in preparing the seaweed sample of *Gracilaria* sp. was to separate it from any impurities. The sample was cleaned, sun-dried, and ground into flour. Proximate analysis of the sample was carried out for its water, carbohydrate, and cellulose content [14]. An illustration of the sample preparation is shown in Fig. 1.

Cellulose isolation

Seaweed powder (100 g) was added into 1 L of 10% (w/v) NaOH, heated at 90–100 °C for 3 h, and filtered. The obtained precipitate was washed until the filtrate pH was neutral. The residue was bleached using 50 mL of 30% (v/v) H_2O_2, heated at 60 °C for 1 h, and filtered. The filtered precipitate was dried in an oven at 60 °C. Chemical analysis of the obtained dried solid was carried out using FTIR. An illustration of the cellulose isolation is shown in Fig. 2.

Synthesis of CA

Cellulose powder (5 g) was diluted in varying amounts of glacial CH_3COOH solution (30, 40, 50, 60, and 70 mL). The sample solution was heated and stirred at 40 °C for 60 min, and then H_2SO_4 2% was added and heated again at 40 °C for 60 min. The mixture solution was added acetic anhydride at 40 °C and stirred for 30 min. The mixture solution was added to 7 mL CH_3COOH and 4 mL of distilled water at 40 °C for 30 min. The mixture solution was left for 2 h, and added

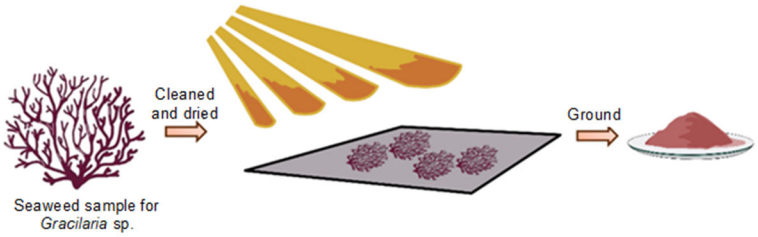

Fig 1. The schematic diagram of sample preparation

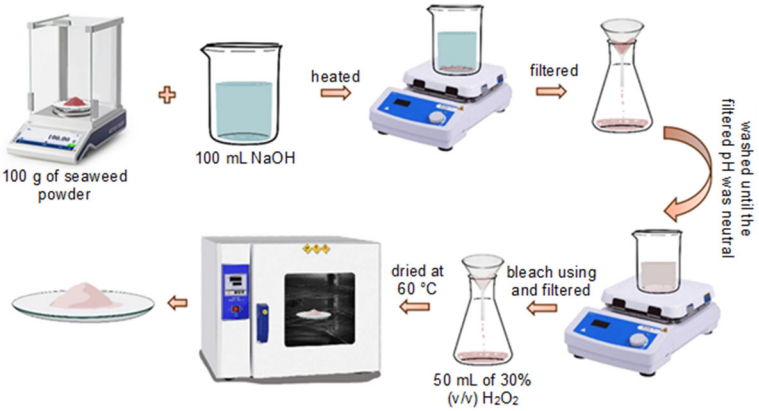

Fig 2. The schematic diagram of cellulose isolation from *Gracilaria* sp.

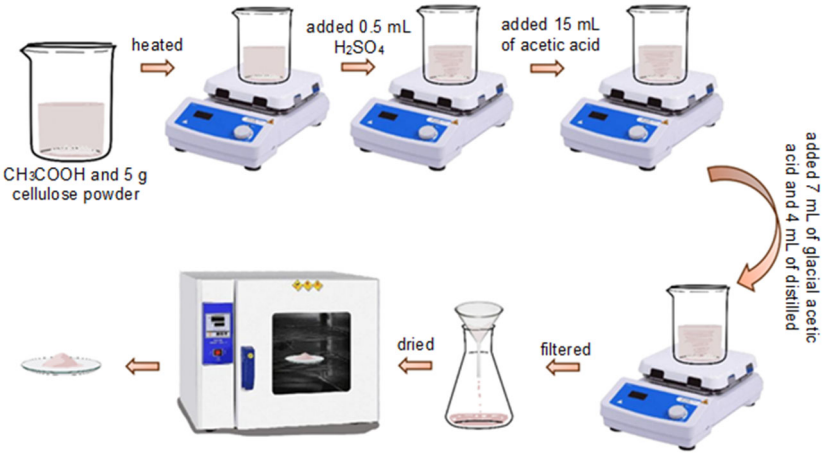

Fig 3. The schematic diagram of the synthesis of CA

with 160 mL of distilled water, and then filtered. Distilled water was used to wash the filtered sediment until the pH reached neutral and the sour smell vanished. The precipitates were then dried at 55 °C. The dried solids were analyzed using an FTIR. An illustration of the CA synthesis is shown in Fig. 3.

CA-NiO electrode film fabrication and its electrochemical properties

The synthesized CA (0.4 g) was added with NiO nanoparticles at 0.0, 0.2, 0.4, and 0.6 g concentrations denoted as (a) CA-NiO0, (b) CA-NiO1, (c) CA-NiO2, and (d) CA-NiO3, respectively. Each mixture was added by 9 mL of DBP. The mixture was heated at 80 °C and stirred at 250 rpm until homogeneous. The mixed solution was poured into the mold until a film was set. The film was analyzed using SEM and XRD to observe its morphological and crystal structures. CV was also used to analyze the electrochemical properties of the electrode.

■ RESULTS AND DISCUSSION

Sample Preparation

Gracilaria sp. sample preparation was carried out to remove contaminants and determine the quality of the materials. The results of the material test analysis can be seen in Table 1. The analysis showed that the water content of *Gracilaria* sp. was 11.31%. The water content for dried seaweed *Gracilaria* sp. was acceptable according to the quality and safety requirements for dried seaweed based on the Indonesian National Standard (SNI) 2690-2015, of which the maximum value is 12%. This means that the *Gracilaria* sp. seaweed powder produced has met SNI standards. Water content dramatically influences the quality of seaweed material. The lower the water content in seaweed, the higher the quality of the seaweed [12]. Meanwhile, the carbohydrate content of the obtained *Gracilaria* sp. was 76.32%. According to SNI 01-2891-1992, the minimum carbohydrate content in dried seaweed is 35.57%. This means that the sample content has met SNI standards. The proximate analysis also found that *Gracilaria* sp. has 16.54% cellulose content (Table 1), whereas according to the previous study, seaweeds have various dry weights of extractable cellulose, which are 9 to 34%. The result shows that the *Gracilaria* sp. sample has potential as the source of cellulose and raw material for CA synthesis.

Characteristics of Cellulose and CA

The cellulose isolation step aims to separate lignin from the cellulose matrix. Because lignin can interfere with the acetylation reaction and the creation of degrees of substitution during the subsequent synthesis of cellulose into CA, thus lignin is undesirable [21]. The FTIR analysis, as depicted in Fig. 4, supports this observation, indicating a decrease in the intensity of the lignin band within the spectral range of 1500 and 1200 cm^{-1}, which corresponds to the lignin carbonyl groups [22]. Where NaOH is used to delignify lignocellulosic materials, this treatment is carried out to disrupt the structure of lignin, where Na^+ ions from NaOH

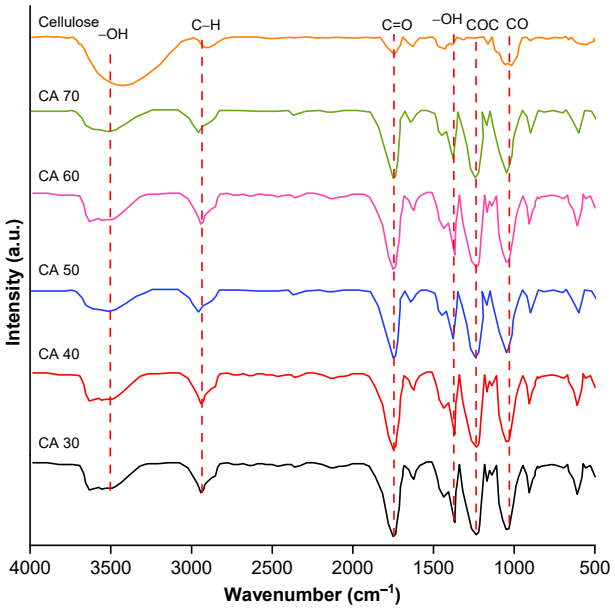

Fig 4. FTIR spectra of isolated cellulose and cellulose acetate with various concentrations of CH_3COOH

Table 1. Material test analysis results

Sample	Water content (% w/w)	Carbohydrate content (% w/w)	Cellulose content (% w/w)
Gracilaria sp.	11.31	76.32	16.54

will bind to lignin to form sodium phenolate, which is polar and easily soluble in water during washing and allows the separation of the structural relationship between lignin and cellulose [23]. The FTIR spectra of cellulose and CA products are shown in Fig. 4. The chemical reaction for separating lignin and cellulose can be seen in Fig. 5.

Fig. 4 also shows the typical absorption of cellulose at a wavenumber intensity of 3423 cm^{-1}, which shows the OH group from the glycosidic bond. In contrast, the CO and $–CH_2–$ groups in the cellulose ring's 1026 and 2900 cm^{-1} regions [24]. Several absorption bands at 1300 to 1400 cm^{-1} indicate the presence of ether groups, which are connected to the carbon chain in cellulose [25]. From the FTIR spectra of synthesized cellulose acetate in Fig. 4. The formation of the acetate group can be confirmed by increasing intensity bands in the 1753–1751 (C=O), 1236 (COO), and 1375–1373 cm^{-1} (CH) regions of the methyl group in acetate [26]. Fig. 4 also shows the hydroxyl group, which was detected at an intensity of 3491–3495 cm^{-1}. This finding indicates that most of the hydroxyl groups originating from cellulose are replaced by acetate groups [27]. The acetylation reaction replaces cellulose hydroxyl groups with acetyl groups, wholly or partially, to produce cellulose acetate products [28]. The protonation and acetylation reaction mechanisms are shown in Fig. 6. Acetylation generally uses acetic acid as a solvent with the help of a sulfuric acid catalyst.

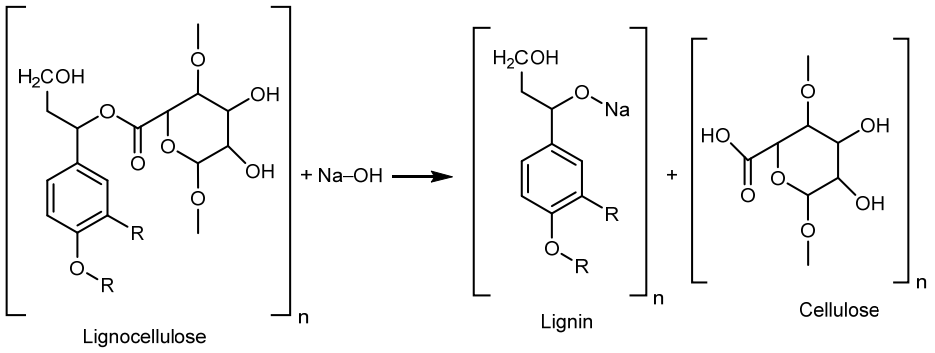

Fig 5. Delignification reaction to separate cellulose from lignocellulose diagram

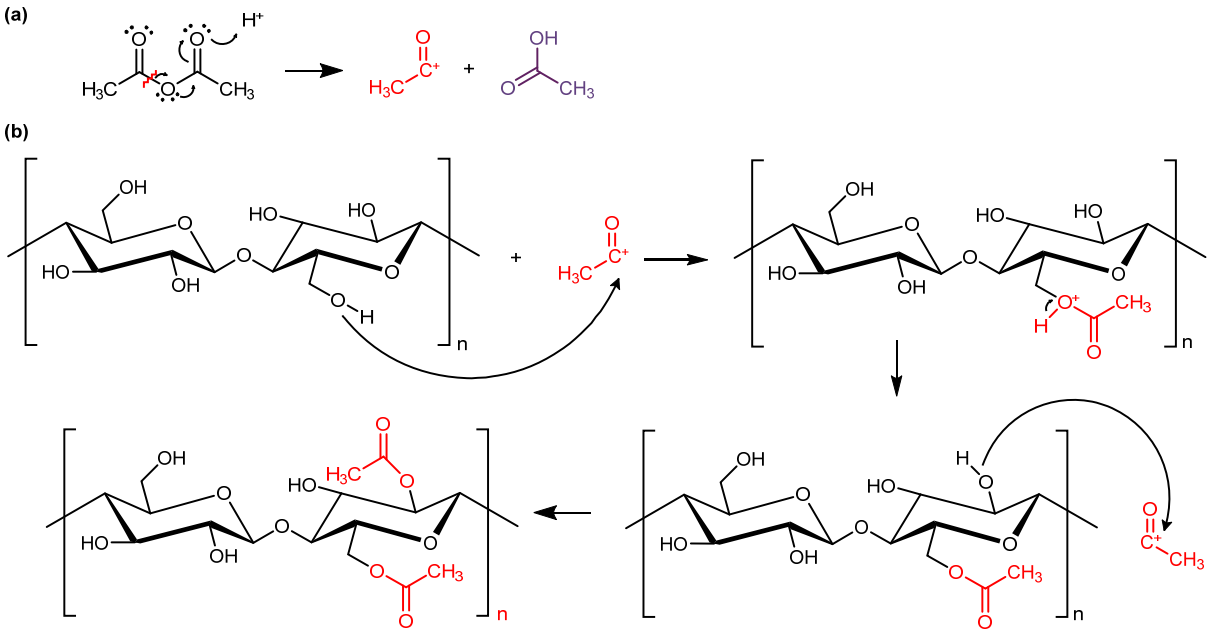

Fig 6. The reactions of (a) the protonation stage and (b) the acetylation stage for cellulose acetate

XRD Analysis of Electrode

The electrode samples were characterized using XRD with a CuKα radiation source (λ = 1.5406 Å) operating at a voltage of 40 kV and a current of 30 mA. Based on the diffractogram in Fig. 7, several characteristic peaks confirm the successful synthesis of CA-NiO in all samples with mass variations. The diffractogram from XRD analysis also shows new peaks in the sample after the addition of NiO. The addition of NiO to CA has reduced the intensity of CA, which can also be seen in Fig. 7, where the CA phase begins to experience a decrease in peak intensity at positions 2θ = 20, 32, and 65°, along with the addition of NiO. The NiO crystal phase was confirmed by the diffraction peaks at typical 2θ values (JCPDS NO. 47-1049) are 37.3, 43.2, and 62.5°, corresponding to the diffraction characteristics (111), (200), and (220) planes of NiO crystals, respectively. No other characteristic peaks are observed from impurities, which shows the CA-NiO has good crystals and purity. The CA-NiO1 up to CA-NiO3 sample has a similar intense peak at 2θ of 37.3, 43.2, and 62.5°. This proves the success of the formation of CA-NiO.

SEM Analysis of Electrode

SEM analysis was used to determine the surface morphology of the CA-NiO electrode with a magnification of 100 times. The results of SEM photo analysis (Fig. 8) show surface images of 4 electrodes, indicating the addition of particles with a larger size on the surface photo both electrodes, where these particles are NiO. The results of SEM analysis can also be used to calculate the porosity value of a material. Porosity is a measure of the space between materials and is the fraction of the volume of space to the total volume; according to the previous study [29], the higher the porosity of electrode material, the higher the specific capacity of the material; this is because porous networks can facilitate ion diffusion over long distances. The porosity value of a material can be calculated by the ratio between volume pore to volume total, which volume pore is calculated by the difference between volume total and volume solid. The porosity of all samples is shown in Table 2. The porosity value of the electrode material increases along with the concentration of NiO. This result shows that apart from doping NiO, it also increases the electrode material's porous area. However, the material's porosity decreased when the NiO concentration was higher than the CA concentration.

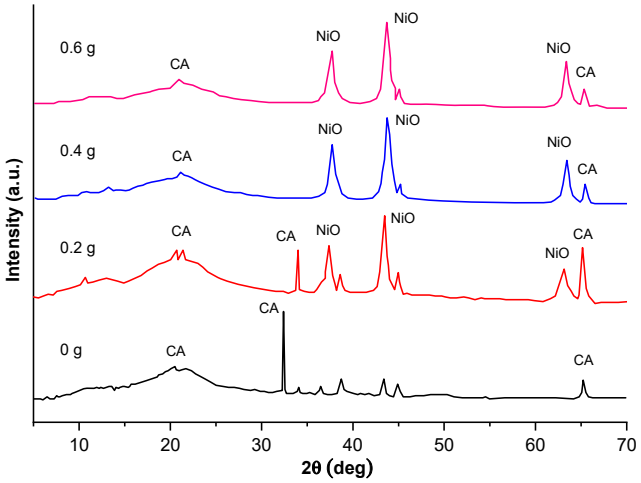

Fig 7. Diffractogram of CA-NiO electrodes with various NiO concentrations

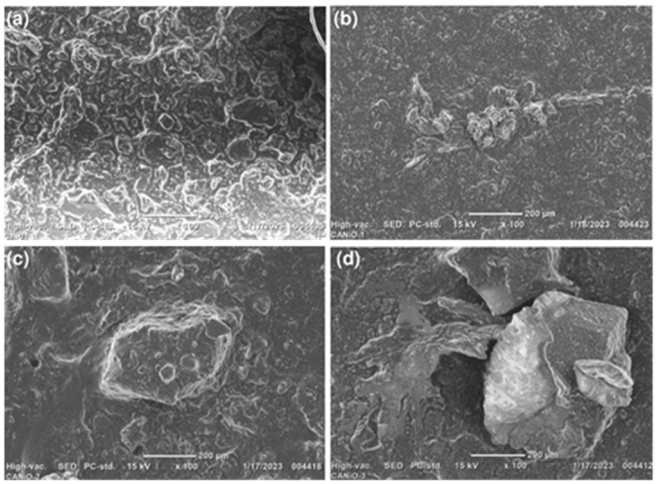

Fig 8. Morphology of CA-NiO electrode with various nickel oxide (a) CA-NiO0, (b) CA-NiO1, (c) CA-NiO2, and (d) CA-NiO3

Table 2. CA-NiO electrode porosity value

Sample code	Mass of CA (g)	Mass of NiO (g)	Porosity (%)
CA-NiO0	0.4	0.0	62.8
CA-NiO1	0.4	0.2	69.1
CA-NiO2	0.4	0.4	72.4
CA-NiO3	0.4	0.6	59.7

The three-dimensional schematic (Fig. S1), converted from SEM data, shows a decrease in solid areas (indicated by the blue regions) with the increasing concentration of NiO added to CA. Therefore, the expanding empty spaces in Fig. S1 are considered porous areas that increase within the electrode material. According to Elango et al. [30], the porous structure significantly enhances the contact area between the electrode and electrolyte ions, which is expected to improve the electrochemical performance of the electrode [30]. In addition, based on the surface morphology of CA-NiO, as shown in Fig. 8, it is clearly seen that there is better pore interconnectivity, which can lead to an increase in the ion diffusion rate and thus improve the voltammetric behavior.

Analysis of Electrochemical Properties of Electrode

Electrochemical properties such as specific capacitance and specific energy of the fabricated electrode samples were analyzed using the CV method, and electrode testing was carried out with scan rates of 10, 20, 50, and 100 mV/s using 0.5 M Na_2SO_4 electrolyte solution. The results of the analysis of the electrochemical properties of the electrode can be seen in Table 3.

The results of potentiostatic CV measurements show the shape of a hysteresis curve (Fig. 9), which indicates that when the cell is applied voltage, a charge storage mechanism occurs due to charge accumulation on the surface of the CA-NiO electrode and 0.5 M Na_2SO_4 electrolyte. The CV hysteresis curve has peaks and valleys that describe the reaction process redox, which is related to the electron handover event on the surface of the CA-NiO electrode. The hysteresis curve demonstrates that the CA-NiO electrode has ideal capacitive properties, allowing it to store electric charge electrostatically by reversibly adsorbing and desorbing electrolyte ions on the electrode surface.

Specific capacitance influences the number of electrons that can be stored under the pressure exerted by an electric current through an oxidation-reduction (Faraday) reaction [31]. The greater the specific capacitance value, the greater the charge stored on the electrode. This charge comes from the accumulation of electrostatic charges on the surface boundaries of the electrodes and electrolytes and results from redox reactions at the electrodes. From the calculation results, as shown in Table 3, the specific capacitance curve for the CA-NiO electrode is obtained, as shown in Fig. 10. The largest specific capacitance occurred in the CA-NiO2 sample at 15500 F/g. The specific capacitance produced in this research is greater than that of previous

Table 3. Analysis of electrochemical properties of CA-NiO electrode

Sample code	Scan rate (mV/s)	Specific capacitance ($\times 10^2$ F/g)	Specific energy ($\times 10^2$ W h/kg)
CA-NiO0	10	6.75	0.58
	20	3.59	0.31
	50	1.44	0.12
	100	0.71	0.06
CA-NiO1	10	8.73	0.75
	20	3.69	0.31
	50	0.96	0.08
	100	0.75	0.06
CA-NiO2	10	15.5	1.33
	20	3.27	0.28
	50	1.21	0.10
	100	0.66	0.05
CA-NiO3	10	2.47	0.21
	20	1.74	0.15
	50	0.88	0.07
	100	0.51	0.04

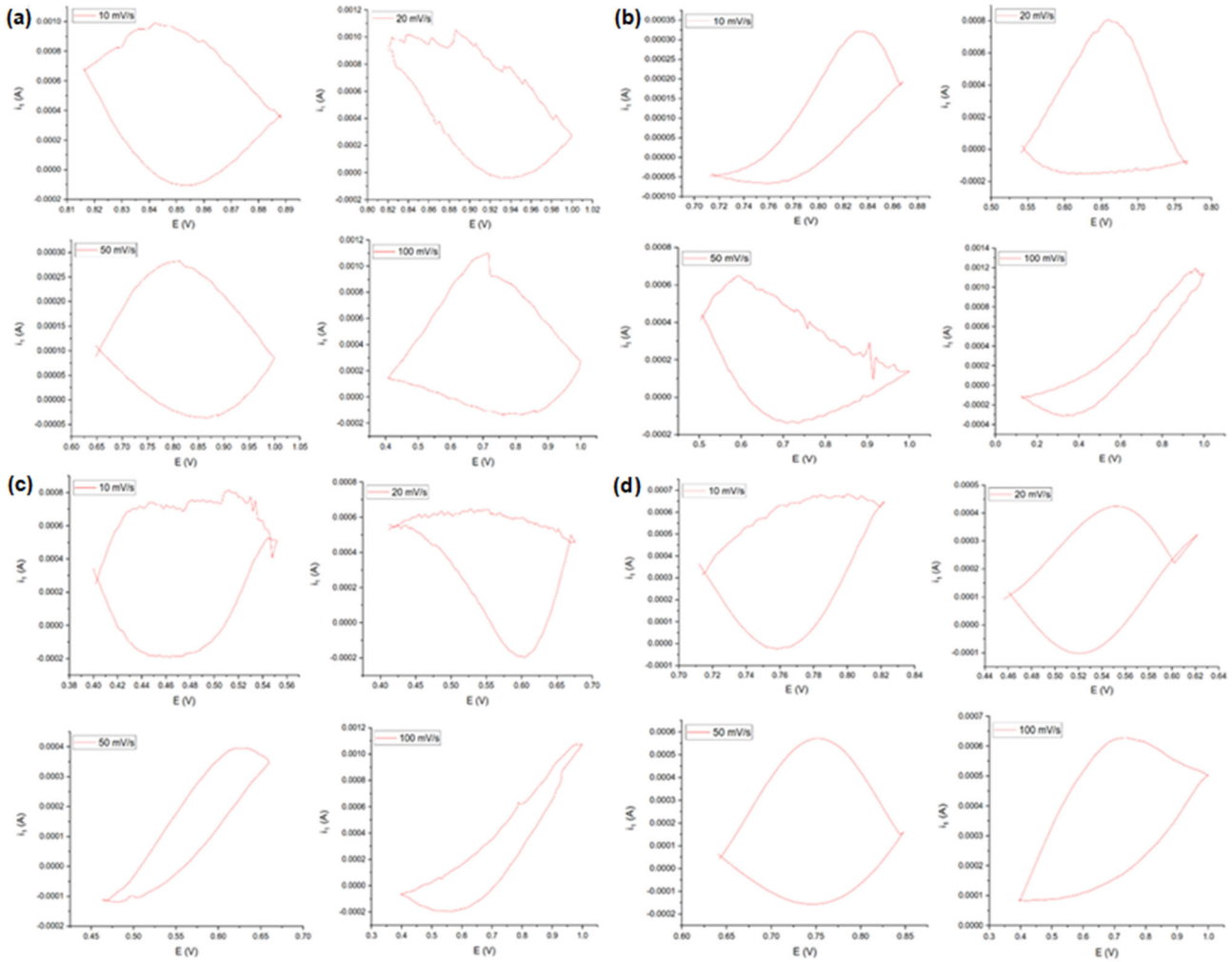

Fig 9. The curve of electrode hysteresis (a) CA-NiO0, (b) CA-NiO1, (c) CA-NiO2, and (d) CA-NiO3

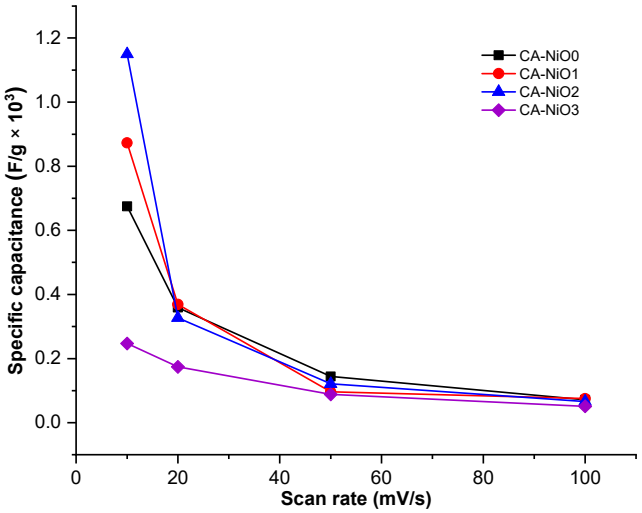

Fig 10. Comparison curve of the specific capacitance of the CA-NiO electrode against changes in scan rate

research that used NiO-carbon composites from banana peel waste in supercapacitor applications [18]. Furthermore, the results obtained were superior to prior research by adding NiO to PAni as a hybrid electrode with a specific capacity of 936 F/g [19].

Specific capacitance analysis was reviewed at the smallest scan rate (10 mV/s) of the particular capacity curve (Fig. 10), where the cell model of the four electrodes shows that the specific capacitance of the CA-NiO0, CA-NiO1, and CA-NiO2 electrodes has increased capacity. Still, for the CA-NiO3 electrode, there has been a definite decrease in the capacity value of the three previous electrodes. This result shows that increasing the NiO concentration in the CA-NiO electrode cell can improve the specific capacitance of the electrode.

According to the previous study's findings [32], adding metal oxide to the electrode film has been shown to enhance the surface area and electron mobility, thereby improving the capacity to store energy.

The decrease in specific capacitance in the CA-NiO3 electrode cell (Fig. 10) shows that when the NiO concentration is higher than CA, it can affect the specific capacitance of the electrode. NiO as a supercapacitor has high theoretical capacitance and low cost [32]. However, its poor electrical conductivity affects its specific capacitance. The decrease in the particular capacitance value on the CA-NiO3 electrode may also be influenced by the reduction of the porosity of the CA-NiO3 electrode (Table 2), which can affect ion diffusion in the CA-NiO3 electrode cell with the electrolyte so that the electrode capacity experiences a specific decrease for the others.

Analysis of Specific Energy

Specific energy analysis was also reviewed at the smallest scan rate (10 mV/s). Based on the Ragone plot diagram (Fig. 11), specific capacitance is directly proportional to a particular energy. This result also correlates with the scan rate value given when measuring CV. When the scan rate is increased to 100 mV/s, the current response on the curve increases, and the time required to complete a CV cycle decreases, indicating that the stored energy is small and the capacity of the CA-NiO electrode is also tiny. Likewise, suppose the scan rate is reduced to 10 mV/s. In that case, the current response that appears in the CV characteristics will also be smaller, so the time required to form a CV cycle will be longer, which indicates that the stored energy is enormous and the electrode capacity is also significant. Thus, the scan rate dramatically influences the power and energy stored in the supercapacitor cell.

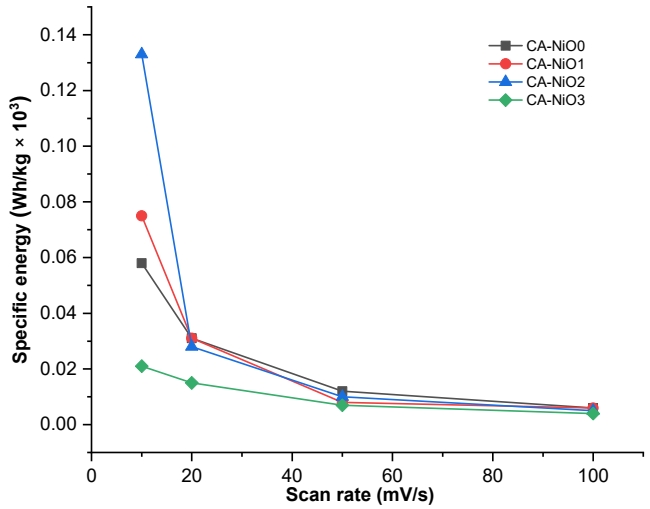

Fig 11. Comparison curve of the specific energy of the CA-NiO electrode against changes in scan rate

■ CONCLUSION

CA was successfully synthesized from cellulose isolated from the algae *Gracilaria* sp., which FTIR spectra analysis proved. The results also show that supercapacitor electrodes have been successfully made where the manufactured electrodes form a composite between CA and NiO, with the highest specific capacitance and specific energy values of 15.5×10^2 F/g and 1.33×10^2 W h/kg, respectively, on the CA-NiO2 electrode, but when the NiO concentration is higher than the CA concentration the specific capacitance and specific energy decrease as shown on the CA-NiO3 electrode. Thus, it can be concluded that CA-NiO synthesized from *Gracilaria* sp. as a raw cellulose material can be used as an electrode in future energy storage and is environmentally friendly. However, further studies are needed on the surface texture properties of the samples using the BET and BJH methods.

■ ACKNOWLEDGMENTS

The authors sincerely thank the dedicated staff at the Biochemistry Laboratory, Department of Chemistry, Faculty of Mathematics and Natural Sciences, Hasanuddin University, Indonesia, for their invaluable support and expertise throughout this research. Additionally, we would like to thank the team at iLab, the Research Center for Biomass and Bioproducts, the National Research and Innovation Agency (BRIN), and the Cibinong Science Center. This research received partial funding from the Institute for Research and Community Services (LPPM) Hasanuddin University through the PFK 2024 fiscal year program under contract No. 00309/UN4.22/PT.01.03/2024.

■ CONFLICT OF INTEREST

All authors declared that there is no conflict of interest.

■ AUTHOR CONTRIBUTIONS

Abdul Karim, Riksfardini Annisa Ermawar, and Ahyar Ahmad designed and supervised the study. Rugaiyah Andi Arfah and Harningsih Karim analyzed the supercapacitor composite and electrochemical properties of the electrodes. Suriati Eka Putri, Andi Erwin Eka Putra, Satria Putra Jaya Negara, Siti Halimah Larekeng, and Ahyar Ahmad performed the experiments, analyzed the data, and wrote the manuscript. All authors have reviewed the manuscript.

■ REFERENCES

[1] Asnawi, R., Nurhadiyanto, D., Arifin, Z., and Asmara, A., 2018, The characteristic of supercapacitors circuit as a future electrical energy storage media, *J. Phys.: Conf. Ser.*, 1140 (1), 012001.

[2] Cao, Q., Zhu, M., Chen, J., Song, Y., Li, Y., and Zhou, J., 2020, Novel lignin-cellulose-based carbon nanofibers as high-performance supercapacitors, *ACS Appl. Mater. Interfaces*, 12 (1), 1210–1221.

[3] Ameen, I., Mishra, R.L., Tripathi, A.K., Siddiqui, A., and Tripathi, U.N., 2020, Photo-physical properties of lanthanides doped *O*-bridged conducting indole oligomer, *Karbala Int. J. Mod. Sci.*, 6 (1), 14.

[4] Wang, M., Liu, K., Dutta, S., Alessi, D.S., Rinklebe, J., Ok, Y.S., and Tsang, D.C.W., 2022, Recycling of lithium iron phosphate batteries: Status, technologies, challenges, and prospects, *Renewable Sustainable Energy Rev.*, 163, 112515.

[5] Subasinghage, K., Gunawardane, K., Padmawansa, N., Kularatna, N., and Moradian, M., 2022, Modern supercapacitors technologies and their applicability in mature electrical engineering applications, *Energies*, 15 (20, 7752.

[6] Bagale, U., Kadi, A., Potoroko, I., Rangari, V., and Mahale, M., 2022, Ultrasound-assisted dibutyl phthalate nanocapsules preparation and its application as corrosion inhibition coatings, *Karbala Int. J. Mod. Sci.*, 8 (2), 3.

[7] Spina, G.E., Poli, F., Brilloni, A., Marchese, D., and Soavi, F., 2020, Natural polymers for green supercapacitors, *Energies*, 13 (12), 3115.

[8] Wang, Q., Liu, W., Yuan, X., Tang, H., Tang, Y., Wang, M., Zuo, J., Song, Z., and Sun, J., 2018, Environmental impact analysis and process optimization of batteries based on life cycle assessment, *J. Cleaner Prod.*, 174, 1262–1273.

[9] Monisha, S., Selvasekarapandian, S., Mathavan, T., Milton Franklin Benial, A., Manoharan, S., and Karthikeyan, S., 2016, Preparation and characterization of biopolymer electrolyte based on cellulose acetate for potential applications in energy storage devices, *J. Mater. Sci.: Mater. Electron.*, 27 (9), 9314–9324.

[10] Teixeira, M.A., Paiva, M.C., Amorim, M.T.P., and Felgueiras, H.P., 2020, Electrospun nanocomposites containing cellulose and its derivatives modified with specialized biomolecules for an enhanced wound healing, *Nanomaterials*, 10 (3), 557.

[11] Wang, J., Song, H., Ren, L., Talukder, M.E., Chen, S., and Shao, J., 2022, Study on the preparation of cellulose acetate separation membrane and new adjusting method of pore size, *Membranes*, 12 (1), 9.

[12] binti Abdul Rahim, K.S., binti Samsuri, A., binti Jamal, S.H., binti Mohd Nor, S.A., binti Rusly, S.N.A., binti Ariff, H., and binti Abdul Latif, N.S., 2023, Redefining biofuels: Investigating oil palm biomass as a promising cellulose feedstock for nitrocellulose-based propellant production, *Def. Technol.*, 37, 111–132.

[13] Chuin Tan, C.H., Sabar, S., Haafiz, M.K.M., Garba, Z.N., and Hussin, M.H., 2020, The improved adsorbent properties of microcrystalline cellulose from oil palm fronds through immobilization technique, *Surf. Interfaces*, 20, 100614.

[14] Baghel, R.S., Reddy, C.R.K., and Singh, R.P., 2021, Seaweed-based cellulose: Applications, and future perspectives, *Carbohydr. Polym.*, 267, 118241.

[15] Zhang, Z., Fang, Z., Xiang, Y., Liu, D., Xie, Z., Qu, D., Sun, M., Tang, H., and Li, J., 2021, Cellulose-based material in lithium-sulfur batteries: A review, *Carbohydr. Polym.*, 255, 117469.

[16] Mousa, H., Abd El-Hay, S.S., El Sheikh, R., Gouda, A.A., El-Ghaffar, S.A., and El-Aal, M.A., 2024, Development of environmentally friendly catalyst Ag-ZnO@cellulose acetate derived from discarded

cigarette butts for reduction of organic dyes and its antibacterial applications, *Int. J. Biol. Macromol.*, 258, 128890.

[17] Hezma, A.M., Labeeb, A.M., and El Desouky, F.G., 2023, Optimizations of performance of cellulose acetate modified by $ZnSnO_3$/ZnO nanocomposites: Electrical, dynamic mechanical analysis, and antibacterial activity, *Colloids Surf., A*, 676, 132110.

[18] Al Kiey, S.A., and Hasanin, M.S., 2021, Green and facile synthesis of nickel oxide-porous carbon composite as improved electrochemical electrodes for supercapacitor application from banana peel waste, *Environ. Sci. Pollut. Res.*, 28 (47), 66888–66900.

[19] Navale, Y.H., Navale, S.T., Dhole, I.A., Stadler, F.J., and Patil, V.B., 2018, Specific capacitance, energy and power density coherence in electrochemically synthesized polyaniline-nickel oxide hybrid electrode, *Org. Electron.*, 57, 110–117.

[20] Nunes, W.G., Da Silva, L.M., Vicentini, R., Freitas, B.G.A., Costa, L.H., Pascon, A.M., and Zanin, H., 2019, Nickel oxide nanoparticles supported onto oriented multi-walled carbon nanotube as electrodes for electrochemical capacitors, *Electrochim. Acta*, 298, 468–483.

[21] Candido, R.G., and Gonçalves, A.R., 2016, Synthesis of cellulose acetate and carboxymethylcellulose from sugarcane straw, *Carbohydr. Polym.*, 152, 679–686.

[22] Meng, F., Wang, G., Du, X., Wang, Z., Xu, S., and Zhang, Y., 2019, Extraction and characterization of cellulose nanofibers and nanocrystals from liquefied banana pseudo-stem residue, *Composites, Part B*, 160, 341–347.

[23] Cui, S., Xie, Y., Wei, X., Zhang, K., and Chen, X., 2022, Exploration of the chemical linkages between lignin and cellulose in poplar wood with 13C and Deuterium dual isotope tracer, *Ind. Crops Prod.*, 187, 115452.

[24] Fahma, F., Lestari, F.A., Kartika, I.A., Lisdayana, N., and Iriani, E.S., 2021, Nanocellulose sheets from oil palm empty fruit bunches treated with NaOH solution, *Karbala Int. J. Mod. Sci.*, 7 (1), 10–17.

[25] Umaningrum, D., Astuti, M.D., Nurmasari, R., Hasanuddin, H., Mulyasuryani, A., and Mardiana, D., 2021, Variation of iodine mass and acetylation time on cellulose acetate synthesis from rice straw, *Indones. J. Chem. Res.*, 8 (3), 228–233.

[26] Hendrawati, H., Liandi, A.R., Ahyar, H., Maladi, I., Azhari, A., and Cornelia, M., 2023, The influence of the filler addition of rice husk cellulose, polyvinyl alcohol, and zinc oxide on the characteristics of environmentally friendly cassava biodegradable plastic, *Case Stud. Chem. Environ. Eng.*, 8, 100520.

[27] Battisti, R., Hafemann, E., Claumann, C.A., Machado, R.A.F., and Marangoni, C., 2019, Synthesis and characterization of cellulose acetate from royal palm tree agroindustrial waste, *Polym. Eng. Sci.*, 59 (5), 891–898.

[28] Sun, X.F., Sun, R.C., and Sun, J.X., 2004, Acetylation of sugarcane bagasse using NBS as a catalyst under mild reaction conditions for the production of oil sorption-active materials, *Bioresour. Technol.*, 95 (3), 343–350.

[29] Milotskyi, R., Serizawa, R., Yanagisawa, K., Sharma, G., Ito, E.R.D., Fujie, T., Wada, N., and Takahashi, K., 2023, Composite of cellulose-nanofiber-reinforced cellulose acetate butyrate: Improvement of mechanical strength by cross-linking of hydroxyl groups, *J. Compos. Sci.*, 7 (3), 130.

[30] Elango, R.K., Sathiasivan, K., Muthukumaran, C., Thangavelu, V., Rajesh, M., and Tamilarasan, K., 2019, Transesterification of castor oil for biodiesel production: Process optimization and characterization, *Microchem. J.*, 145, 1162–1168.

[31] De, P., Halder, J., Gowda, C.C., Kansal, S., Priya, S., Anshu, S., Chowdhury, A., Mandal, D., Biswas, S., Dubey, B.K., and Chandra, A., 2023, Role of porosity and diffusion coefficient in porous electrode used in supercapacitors – Correlating theoretical and experimental studies, *Electrochem. Sci. Adv.*, 3 (1), e2100159.

[32] Fu, X., Wen, J., Xia, C., Liu, Q., Zhang, R., and Hu, S., 2023, Nafion doped polyaniline/graphene oxide composites as electrode materials for high performance flexible supercapacitors based on Nafion membrane, *Mater. Des.*, 236, 112506.